Scientia Iranica A (2014) 21(4), 1263–1280

Sharif University of Technology
Scientia Iranica
Transactions A: Civil Engineering
www.scientiairanica.com

Rate-dependence of rockfill behavior on propagated near fault ground motions

H.R. Razeghi[a], A. Aghaei Araei[b,*], A. Ghalandarzadeh[c] and S. Hashemi Tabatabaei[d]

a. *School of Civil Engineering, Iran University of Science and Technology (IUST), Narmak, Tehran, P.O. Box 16765-163, Iran.*
b. *Geotechnical Engineering Laboratory, Road, Housing and Urban Development Research Center (BHRC), Tehran, P.O. Box 13145-1696, Iran.*
c. *School of Civil Engineering, College of Engineering, University of Tehran, P.O. Box 11365-4563, Iran.*
d. *Department of Geotechnical Engineering, Road, Housing and Urban Development (BHRC), Tehran, P.O. Box 13145-1696, Iran.*

Received 9 December 2012; received in revised form 5 August 2013; accepted 15 October 2013

KEYWORDS
Triaxial;
Rockfill;
Frequency;
Modulus;
Damping;
Spectra.

Abstract. Equivalent linear one-dimensional site response analysis, which approximates nonlinear soil behavior within the linear analysis framework, is widely used in estimating local site effects. In this analysis, soil behavior is often assumed to be independent of the frequency of seismic loading. However, the large scale triaxial test results on rockfill material have shown that the shear modulus and, especially, the damping ratio, are influenced by the loading frequency. A series of one-dimensional equivalent linear analyses were performed on 30 m and 90 m thick profiles of the studied rockfill material to evaluate the frequency-dependent soil behavior under several well-known near-fault ground motions. The analyses are carried out for three base acceleration levels, namely, 0.1 g, 0.35 g and 1 g, using the simple time history scaling method. Results show that the frequency-dependent shear modulus and damping ratio can have a pronounced influence on propagated ground motion. The frequency-dependent soil behavior is also dependent on the thickness of the soil profile, amplitude, equivalent no. of cycles at $0.65\tau_{\max}$, and frequency content of the input ground motion.

1. Introduction

One-dimensional site response analysis is widely performed to account for local site effects during an earthquake [1,2]. The main deficiency of the procedure is constant application of the shear modulus and damping throughout the analysis selected at the effective shear strain. Moreover, it is shown that the dynamic and damage behavior of geo-structures is highly sensitive to the frequency content of ground motion [3,4]. Frequency-dependent equivalent linear procedures were proposed to overcome such limitations and better simulate the nonlinear soil behavior [5-8]. This procedure is based on the observation that the amplitude of shear strain decays quickly with an increase in frequency. Such observations led to development of equations of frequency-dependent shear strain. The equations are essentially smoothed curves of the Fourier spectra of shear strain time histories of earthquakes. The analyses performed by Kwak et al. [9] show that the frequency-dependent algorithm proposed by Yoshida et al. [7] and Assimaki and Kausel [8] do not always improve the accuracy of the solution. Generally, the frequency-dependent procedures can,

*. *Corresponding author. Tel.: +98 21 88255942; Fax: +98 21 88255942*
E-mail addresses: razeghi@iust.ac.ir (H.R. Razeghi); aghaeiaraei@bhrc.ac.ir (A. Aghaei Araei); aghaland@ut.ac.ir (A. Ghalandarzadeh); htabatabaei@bhrc.ac.ir (S. Hashemi Tabatabaei)

especially, result in unrealistic amplification of low period components using a ground motion rich in high frequency content. Selection of G and D curves independent of testing loading frequency may be responsible for the deficiency. The reason for considering frequency dependency is that the behavior is considered over the whole duration of the earthquake, but the strain rate dependency codes, such as FDEL [5] and DYNEQ [7], assign different material properties to different Fourier series components of the shear strain. Similar to SHAKE 91 [10] and EERA [11], FDEL and DYNEQ determine modulus and damping ratio that are maintained constant throughout the shaking, although each Fourier component has different modulus and damping ratio.

Dynamic parameters of gravels are affected by various factors like the confining pressure or the loading frequency. For modeled rockfill, such a dependency is not explicitly modeled and completely understood.

In contrast to common practice in geotechnical earthquake engineering [12], recent studies [13-35] show that shear modulus and damping ratio are dependent on the frequency of loading.

It is observed that, in general, G and D values increase as loading frequency increases. Moreover, at certain strain, $G/G_{\max}$ ratio decreases, as loading frequency is increased.

The high values of damping for all strain ranges studied at loading frequencies of 5 Hz and 10 Hz of the rockfill material with low void ratio may be attributed to the sensitivity of their structure to loading frequency. This is due to increased collision of soil particles, resulting in the high dissipation of energy at contact points of the particles [16,26,30]. Also, in discrete rockfill material, due to the time-lag between a driven cyclic stress and the driven strain in these large triaxial specimens, the effect of frequency is to increase both modulus and damping ratio. The effect of inertia on individual rockfill particles is to reduce the modulus and increase damping ratio [16]. The net effect of frequency is to increase the damping in particle contact, while it has less pronounced effect on shear modulus.

Owing to the limited available data for fine grain and sand soils at low shear strains, Meng [22] and Park and Hashash [36] assumed that only the small strain modulus and damping are frequency dependent. However, the frequency-dependent dynamic soil properties, even at low strain, are not explicitly modeled.

The paper studies the effect of frequency content on the shear modulus and damping ratio behavior at wide range of strains using available data obtained from large scale triaxial tests on modeled gravelly rockfill material. The previous published results by the authors were implemented and evaluated in a one dimensional equivalent linear site response analysis, at the specified sites, to evaluate the effect of the frequency-dependent soil behavior on propagated ground motion under several well-known near-fault ground motions.

2. Frequency-dependent gravelly soil behavior via laboratory testing

2.1. Material properties

In this study, the tested gravelly rockfill samples were obtained from the shell materials of the under construction upper Siah-Bisheh High Concrete Faced Rockfill Dam (CFRD) in Iran. The limestone rockfill material was produced by quarry blasting, and the particles were very angular. The above type of material will hereinafter be referred to as S.SBU in the paper. Table 1 summarizes the main characteristics of the material and testing program, including rockfill name, size distribution, point load strength index, Los Angeles abrasion, dry density, optimum water content, specific gravity, minimum void ratio (e_o), range of confining pressures and loading frequencies. The gradation curve of the material for triaxial testing was obtained with maximum particle sizes of 50 mm (1/6 the diameter of the large-scale triaxial specimen, which is 30 cm. See Figure 1). D_{10}, D_{30}, D_{50} and D_{85} values are 0.5, 2.5, 6.5 and 25 mm, respectively. S.SBU material consists of 3.8% fine grains and the passing percentage from sieve No. 4 (4.75 mm) is equal to 42%. The maximum dry densities are estimated according to the

Table 1. Characteristics of gravelly materials and testing program according to ASTM D3999.

Material symbol	S.SBU
Gs (Bulk specific gravity - oven dry) (ASTM C127)	2.71
$e_{\min}$	0.161
Maximum particle size (mm)	50
$D_{10}, D_{30}, D_{50}, D_{85}$ (mm)	0.5, 2.5, 6.5, 25
Passing #200 (%)	3.8
Point load index (Is)*	3.07
Loss Angeles abrasion for no. of rotations of 500 (%) (ASTM C131)	40
ASTM D1557 $\gamma_{d(\max)}$ (gr/cm^3)	2.29
(C-method) (%) ω_{opt}	5.33
Dimension of samples (cm)	30 cm (diameter)*60 cm (height)
σ_3' (kg/cm^2)	1, 2, 4, 6, 10, 15
Frequency of loading (Hz)	0.1, 0.2, 0.5, 1, 2, 5, 10

*: ISRM

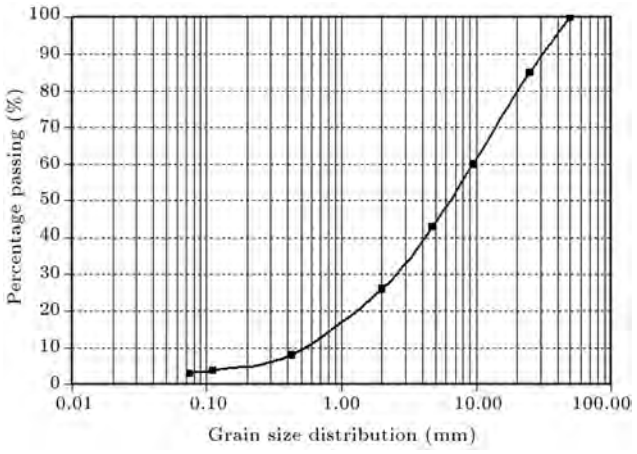

Figure 1. Grain size distribution for modeled rockfill material in triaxial testing.

ASTM D1557 (C-method) [37] for portions smaller than 19 mm and modified for oversize (20% higher than 19 mm) percentages [38]. The value of maximum dry densities is 2.29 gr/cm^3. The specimens were prepared according to the maximum dry density of 2.15 gr/cm^3.

Axial loads, vertical displacements, volume changes and pore pressures were measured at periodic intervals of 0.2, 0.1, 0.04, 0.02, 0.01, 0.004 and 0.002 seconds, respectively, for the applied sinusoidal load, with frequencies of 0.1, 0.2, 0.5, 2, 5 and 10 Hz in undrained conditions. Tests results, including the shear modulus and damping ratio versus shear strains, have been calculated based on the stress-strain hysteresis loop for the 1 to 40th cycles, according to ASTM D3999 [39]. More details about the characteristics of S.SBU gravelly material, dynamic testing program, accuracy of measurements, testing procedure for determination of the modulus, and the damping properties of the 42 specimens using the cyclic triaxial apparatus [39], can be found in [33].

2.2. Frequency-dependent shear modulus, G/G_{max} relationship and damping ratio

Generally, at low strain amplitudes, the shear modulus is nearly constant and at its highest value, G_{max}, but, it decreases while the strain amplitude is increasing. In this study, the extrapolation method was employed from 0.0001% strain to obtain G_{max} for the material [33].

Moreover, it is necessary to define the soil model by equations obtained from data interpolation. For example, Figure 2 shows the variation of $G_{max(f)}/G_{max(f=0.1\ Hz)}$ ($G_{max(f=0.1\ Hz)}$ = maximum shear at loading frequency of 0.1 Hz) versus loading frequency at different confining pressures for S.SBU material. Results indicate that there is not a unique correlation, and definition of the full behavior requires a set of parameters for each confining pressure.

Figure 3 shows the G/G_{max} versus γ relations

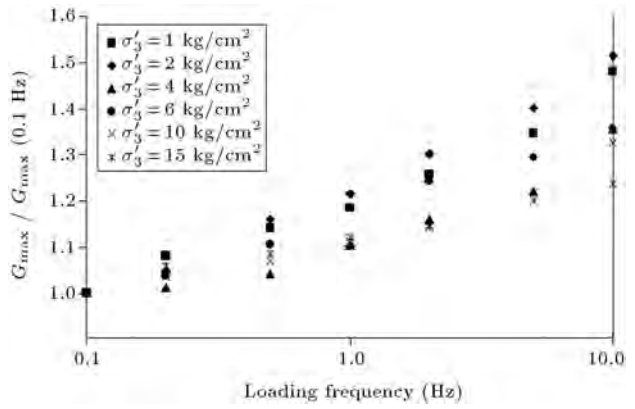

Figure 2. Variation of G_{max}/G_{max}(0.1 Hz) versus loading frequency at different confining pressures for S.SBU material.

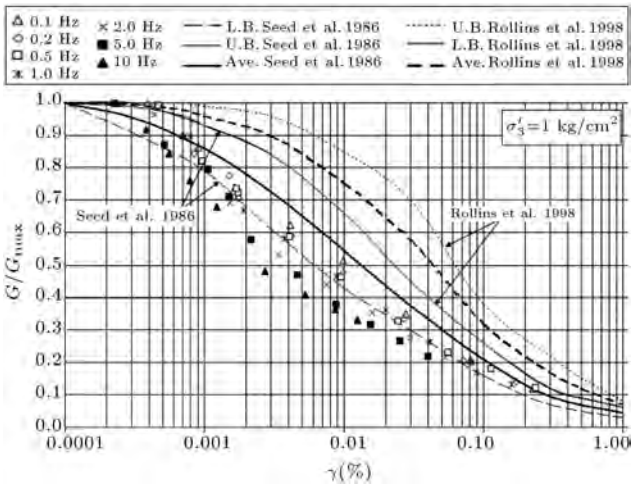

Figure 3. G/G_{max} versus γ relations at different loading frequencies and confining pressure of 1 kg/cm^2 for S.SBU material.

at different loading frequencies and confining pressure of 1 kg/cm^2 for S.SBU material. Similarly, a set of parameters for each confining pressure is required.

Figure 4 presents damping ratio versus γ at different loading frequencies and confining pressure of 1 kg/cm^2 for S.SBU material. Generally, the damping ratio versus shear strain of the studied rockfill materials, under loading frequency of 0.1 Hz, falls almost in the range identified by Rollins et al. [40]. However, at higher loading frequencies (5 and 10 Hz), the damping ratios fall completely above the upper bound trend observed by Seed et al. [41].

Figure 5 shows the frequency-dependent damping ratio at two shear strain levels, 0.01% and 0.001%, for confining pressure of 1 and 4 kg/cm^2 in S.SBU rockfill material. The ratio of $D/D_{(f=0.1\ Hz)}$ ($D_{(f=0.1\ Hz)}$ =damping at loading frequency of 0.1 Hz) versus frequency has considerable variations by increasing confining pressure and shear strain amplitude. It is not possible to obtain a unique model from exper-

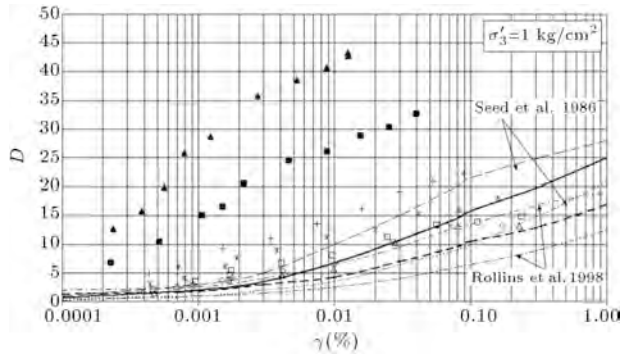

Figure 4. Damping ratio versus γ at different loading frequencies and confining pressure of 1 kg/cm^2 for S.SBU material.

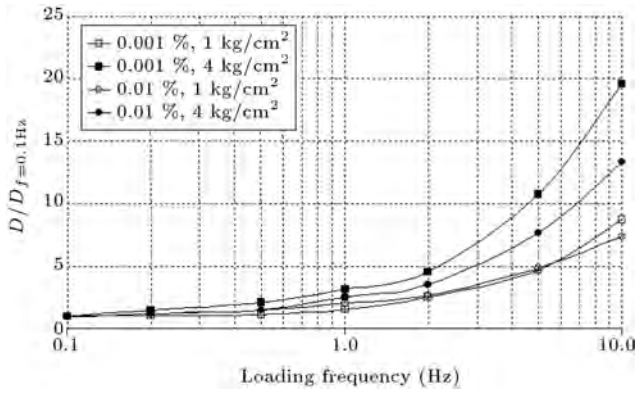

Figure 5. Frequency-dependent damping ratio behavior at two shear strain levels of 0.01% and 0.001% for confining pressure of 1 and 4 kg/cm^2 for S.SBU rockfill material.

imental data representing the pressure and frequency dependency of G and D on shear strain. Therefore, this study uses curves developed for loading frequency to perform a site response analysis subject to broadband seismic motion.

3. Influence of frequency-dependent soil behavior on site response analysis

In the above sections, a comprehensive study of the frequency-dependent dynamic properties (i.e., shear modulus and damping ratio) of a rockfill material, with the aid of large scale triaxial equipment, was presented. Although the amplification factor at ground surface, with respect to the frequency-dependent dynamic properties of rockfill materials, under different near-fault motions with different velocity periods, is recognized, it is not well characterized and quantified. In current building codes [42,43,44], the upper 30 m of surface soil deposits overlying the higher impedance earth crust are regarded as the most relevant and significant in characterizing the seismic behavior of a site. Due to extensive usage of high compacted rockfill material, and a limitation of suitable one dimensional site responses available for near-fault ground motion results, it is useful to carry out investigations for obtaining amplification and spectral acceleration for 30 m and even thicker (e.g. 90 m, which is the height of a CFRD under construction in Iran) in order to have economical, safe designs and constructions. However, in the case of a rockfill dam, compared to 1D analysis (which is useful for level or gently sloping sites with parallel material boundaries), a 2D analysis is more appropriate.

4. Frequency-dependent behavior in equivalent linear analysis

A simplified equivalent linear analysis procedure [10,11], which is modified by Sugito [6], was used to approximate the frequency-dependent soil behavior.

According to the Frequency-Dependent Equivalent Linearized (FDEL) technique, the frequency-dependent equivalent strain is proposed in the following equation [6]:

$$\gamma_{eff}(\omega) = C\gamma_{\max}\frac{F_a[\gamma(\omega)]}{F_a(\gamma_{\max})}, \tag{1}$$

where $\gamma_{\max}$ is the maximum shear strain, $F_a[\gamma(\omega)]$ is the Fourier spectrum of shear strain, and $F_a(\gamma_{\max})$ represents the maximum of $F_a[\gamma(\omega)]$. The definition of γ_{eff} in the left side of equation (1) is described, where the equivalent strain, which controls equivalent shear modulus and damping factor, is given in proportion to the smoothed spectral amplitude of shear strain in the frequency domain. The constant, C, controls the level of equivalent strain uniformly along the frequency axis. Typically, this ratio ranges from 0.4 to 0.75, depending on the input motion and magnitude. The following equation may be used to estimate this ratio [10]:

$$C = (M-1)/10, \tag{2}$$

where, M is the magnitude of the earthquake. For example, for $M = 6.7 - 7.6$, the ratio would be $0.57 - 0.66$. Sugito [6] suggests $C = 0.65$ as a relevant value.

The equivalent linear model specified the variation of shear modulus and damping ratio with frequency-dependent equivalent strain amplitude, which is used in SHAKE 91 [10].

It assumes that the complex shear modulus (G^*) is a function of the critical damping ratio, ξ ($\xi = \omega\mu/2G$, where η is the viscosity, $\omega = 2\pi f$ is angular frequency, and f is frequency), and real shear modulus (G) as follows:

$$|G^*| = G\sqrt{1+4\xi^2}, \tag{3}$$

which implies that $|G^*|$ increases with ξ. Figure 6 shows the variation of $|G^*|/G$ with ξ; the ratio can be as much as 1.35 when ξ reaches 45%.

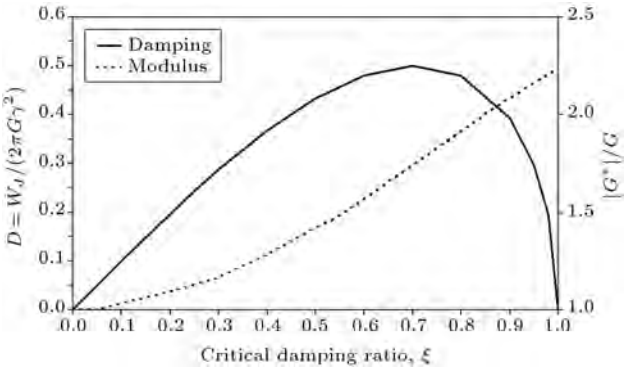

Figure 6. Variations of damping ratio and normalized complex shear modulus amplitude as a function of critical damping ratio ξ ($\xi = \pi f\mu/G$).

The energy dissipated during a loading cycle is:

$$W_d = 2\pi G\xi\sqrt{1-\xi^2}\gamma^2. \tag{4}$$

Then damping ratio is calculated as:

$$D = W_d/2\pi(W_s) = 2\pi G\xi\sqrt{1-\xi^2}\gamma^2/2\pi(2^*0.5^*G\gamma^2). \tag{5}$$

Figure 6 shows the variation of damping ratio with ξ. The damping ratio is dependent on ω, and increases linearly with ξ to less than 25%. Moreover, the damping ratio of the model reaches a plateau at ξ around 0.5 and then tends toward zero at $\xi = 1$.

After getting $\gamma_{eff}(\omega)$, damping ratio and shear modulus can be evaluated from the cyclic shear deformation characteristic test results, so called, $D-\gamma$ and $G-\gamma$ relationships. Only one set of $D-\gamma$ and $G-\gamma$ curves were used for a soil at a given layer. Iterative approximation of equivalent linear response in the FDEL is similar to SHAKE [45]. However, there is a main difference; strain dependency characteristics by SHAKE are, of course, constant values of shear strain, damping and modulus at all ranges of studied frequencies.

Moreover, the author's suggestion for improvement of the FDEL technique (i.e. unrealistic amplification of low period components using a ground motion rich in high frequency contents) can be summarized as follows:

i. For the selected ground motion, a predominant frequency was calculated.

ii. FDEL analyses were performed for rockfill material tested at different loading frequency ranges between 0.1 and 10 Hz in order to obtain upper and lower bound responses.

iii. The response related to the behavior curves of materials in coincidence with the predominant frequency of the considered earthquakes from the available results was selected. This means the selection of $G_{\max}$ values, $G/G_{\max}$, and D curves with reference to the dominant frequency (we consider the dominant frequency of the input motion).

iv. In the case of frequency-independent rockfill behavior, the testing frequency of the dynamic curve for different predominant frequencies of input ground motion was assumed to be 0.1 Hz.

v. For comparison, the spectral acceleration ratio, the results of step iv, must be compared with the results of step iii.

This means, a number of analyses with different parameters should be carried out by using the FDEL code.

In the frequency domain solution, applying the boundary condition results in the following recursive formula between the motion of two subsequent layers, n and $n+1$:

$$A_{n+1} = \frac{1}{2}A_n(1+\alpha_n^*)\exp ik_n^*h_n + \frac{1}{2}B_n(1-\alpha_n^*)\exp -ik_n^*h_n, \tag{6}$$

$$B_{n+1} = \frac{1}{2}A_n(1+\alpha_n^*)\exp ik_n^*h_n + \frac{1}{2}B_n(1-\alpha_n^*)\exp -ik_n^*h_n, \tag{7}$$

where $A_{n+1}(W)$ and $B_{n+1}(W)$ are the upward and downward components of the ground motion of layer $n+1$, respectively, $a_n^* = \frac{\rho_n[\sqrt{G_n(\omega)/\rho_n}]_n[1+iD_n(\omega)]}{\rho_{n+1}[\sqrt{G_{n+1}(\omega)/\rho_n}]_{n+1}[1+iD_{n+1}(\omega)]}$ is the complex impedance ratio, $k_n^* = \frac{\omega}{[\sqrt{G_n(\omega)/\rho_n}]_n[1+iD_n(\omega)]}$ is the complex wave number, ρ is the density, $G(\omega)$ is the shear modulus and $D(\omega)$ is the damping ratio. The equivalent linear analysis uses the transfer function, which is defined as the Fourier spectral ratio of input motion to the output motion, to simulate ground vibration. Setting the displacement at the surface as 2, the transfer function that relates an input motion imposed at bedrock to the surface motion is as follows:

$$F(\omega) = \frac{|u_{\text{surface}}|}{|u_{\text{input motion}}|} = \frac{2}{A_{\text{Bedrock}}(\omega)+B_{\text{Bedrock}}(\omega)}, \tag{8}$$

in which u_{surface} is the displacement at the surface and $u_{\text{input motion}}$ is the displacement of the input ground motion. The transfer function accounts for the variation in the shear modulus and damping ratio of each layer of the soil profile, depending on the loading frequency of the input ground motion.

5. Characteristics of near-fault input ground motions and site response analysis

In this study, several well known near-fault motion records are used in the response analysis. Near-fault earthquakes records were selected from the strong motion database of the Pacific Earthquake Engineering Research Center (http://peer.berkeley.edu/) [46] and Iran Strong Motion Network (ISMN) for specific reasons of location of the rockfill site.

The selected ground motions are listed in Table 2. Their maximum recorded acceleration ranges from 0.25 g to 1 g, and the predominant frequency ranges between 1 and 13 Hz. The equivalent no. of cycles at $0.65\tau_{\max}$ [47] ranges between 2 and 26. The earthquakes selected for comparison have occurred over hundreds of years during the past. Figure 7 presents an example of longitudinal time-history components for Bam and Landers earthquakes, as well as their spectral accelerations. One of the main characteristics of near-fault records is that the maximum amplitude of the relative velocity spectrum increases as predominant frequency decreases (Figure 8). The two horizontal components of ground motion presented in Table 2 were used as an input motion imposed at the bedrock in a horizontal direction. The vertical component was also used to get the spectra of the vertical component of motion (Table 2). The 30 and 90 m thick profiles were used in the analyses. The S.SBU dynamic properties at different stresses and frequencies were used in the analyses [33]. The model is implemented in the computations, as explained below:

- $G_{\max}$ is increased with depth for each sub-layer.
- $G/G_{\max}$ and D decay curves are selected according to the depth.

For bedrock (at a depth of 30 m or 90 m), in all analyses, Idriss [2] normalized shear modulus and damping ratio curves were used (Figure 9). Analyses were carried out at three different levels of base accelerations, namely, 0.1, 0.35 and 1 g, so that the earthquake time-history is scaled in a simple manner, with respect to the desired maximum base accelerations. Scaling the earthquake was carried out because responses at the serviceability state and ultimate limit state were considered.

Totally, 1296 analyses have been carried out for assessing the amplification, spectral acceleration, normalized spectral acceleration (B), spectral acceleration ratio (ratios between the rate-dependent and

Table 2. Input near-fault motions used in site response analysis.

Earthquake	Mag.[a]	Hypocenter depth (km)	Station	Closest distance to epicenter (km)	$\bar{V}s(30)$ (m/s)[b] of accel.[c] station	Peak acceleration/ predominant frequency equivalent no. of cycles at $0.65\tau_{\max}$/ duration(s)[d]		
						Normal (L) component	Parallel (T) component	Vertical (V) component
Chi-Chi, 1999-09-20	7.62	6.8	CWB 99999 CHY080	2.69	533	0.968g/ 1.508 Hz/3/16	0.902g/ 1.424 Hz/2/13	0.724g/ 2.774 Hz/2/8
Kobe, 1995-01-16	6.90	17.9	JMA 99999 KJMA	0.96	312	0.821g/ 2.024 Hz/5/19	0.59 9g/ 2.007 Hz/7/15	0.343g/ 3.606 Hz/13/16
Tabas, 1978-09-16	7.35	5.8	9101 Tabas	2.05	767	0.852g/ 3.841 Hz/11/34	0.8 36g/ 4.000 Hz/13/32	0.689g/ 7.112 Hz/11/27
Landers, 1992-06-28	7.28	7.0	SCE 24 Lucerne	2.19	684	0.721g/ 9.422 Hz/21/16	0.7 85g/ 10.482 Hz/15/16	0.819g/ 13.007 Hz/26/16
Northridge, 1994-01-17	6.69	17.5	DWP 77 Rinaldi Receiving Sta.	6.50	282	0.838g/ 2.282 Hz/6/13	0.47 4g/ 3.650 Hz/17/13	0.852g/ 7.886 Hz/9/11
Bam, 2003-12-26	6.7	5	Farmandari	< 1	422	0.799g/ 4.862 Hz/15/26	0.636g/ 5.077 Hz/13/23	0.999g/ 8.378 Hz/11/23
Erzincan, 1992-03-13	6.9	9	95 Erzincan	4.38	275	0.515g/ 1.396 Hz/2/13	0.496g/ 2.249 Hz/4/13	0.248g/ 5.546 Hz/8/12
Duzce, 1999-11-12	7.1	10	Duzce	6.58	276	0.535g/ 2. 156 Hz/4/14	0.348g/ 1.928 Hz/13/14	0.357 g/ 8.435 Hz/10/12
Average [peak acceleration (g) / predominant frequency (Hz)/ no. cycles/duration(s)]						0.756/3.436/8/19	0.634/3.852/10/17	0.629/7.093/11/16

[a]: Mag.: Magnitude; [b]: Average $\bar{V}s(30) = 378$ m/s; [c]: accel.: acceleration; [d]: Based on threshold acceleration of 0.05 g.

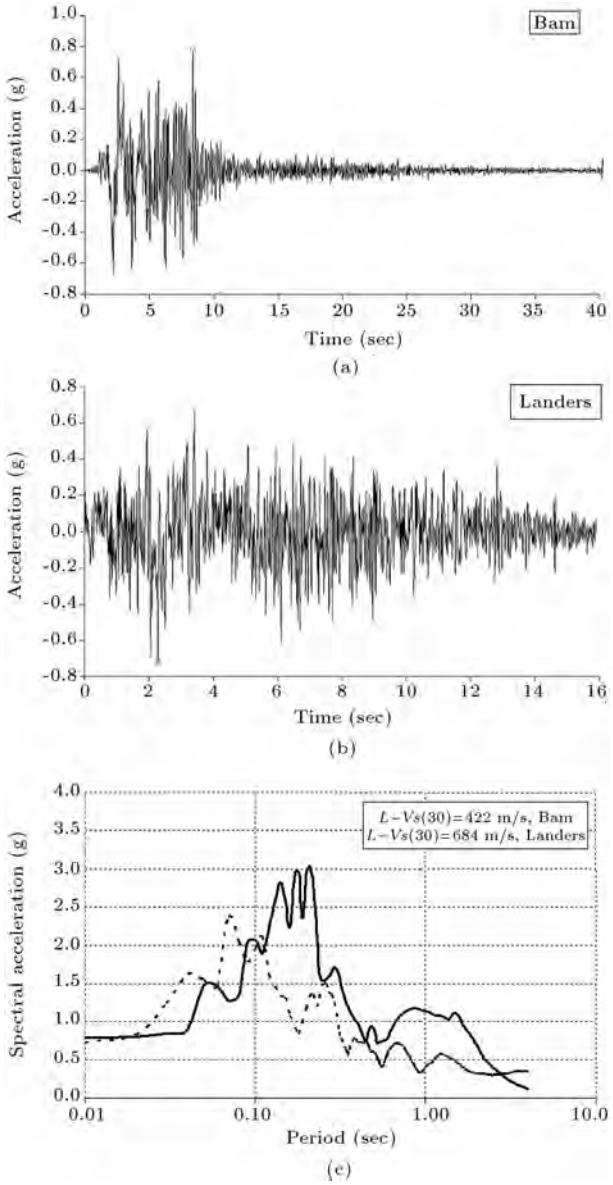

Figure 7. Example of used earthquakes (longitudinal-component) in the analyses: (a) Bam time history; (b) Landers time history; and (c) spectral acceleration.

rate-independent spectral accelerations, where the frequency of the dynamic curves in the case of rate independent was assumed to be 0.1 Hz), spectral relative velocity, and spectral relative displacement parameter at the ground surface. Soil layers at the near surface were divided into 1.5 to 2 meter portions, and at a greater depth to 3 m. For each layer, suitable properties were selected based on depths and stress levels. Unit weight at the ground surface was assumed to be 21.5 kN/m^3, and the bedrock to be 22.9 kN/m^3.

The shear wave velocity was calculated based on the $G_{\max}$ value of the triaxial testings (Table 3). The $\bar{V}s(30)$ of the 30 m and 90 m thick rockfill are 378 m/s and 534 m/s, respectively. The minimum, average,

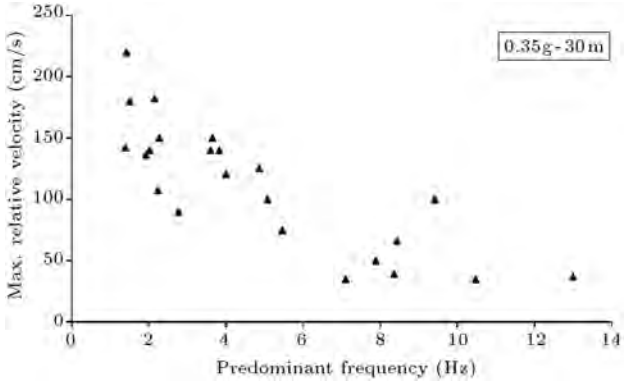

Figure 8. Maximum relative spectrum velocity versus predominant frequency for near-fault records under 0.35 g bed rock acceleration and 30 m thick soil column.

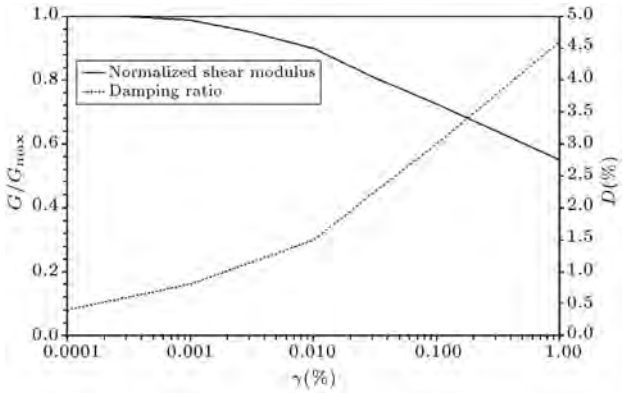

Figure 9. Curves for dynamic behavior of bedrock (Idriss 1990).

Table 3. Results of tests to determine $V_{\max}$ (m/s) for S.SBU material.

Loading frequency (Hz)	σ_3' (kg/cm^2)	1	2	4	6	10	15
	0.1	331	355	464	534	591	712
	0.2	344	362	467	543	600	731
	0.5	354	382	473	561	610	741
	1	360	391	487	581	622	753
	2	371	405	499	595	632	760
	5	384	420	512	607	651	779
	10	403	437	540	621	680	791

and maximum values of normalized shear modulus and damping ratio from laboratory tests by [40,41] were used with respect to stress levels in the analyses.

The number of iterations used in the analyses is 8 to ensure convergence. The surface response spectra for SDOF (single degree of freedom) have been computed for 5% damping.

5.1. Results for 30 m thick profile

A set of analyses was performed to evaluate the effect of frequency dependency of the shear modulus and

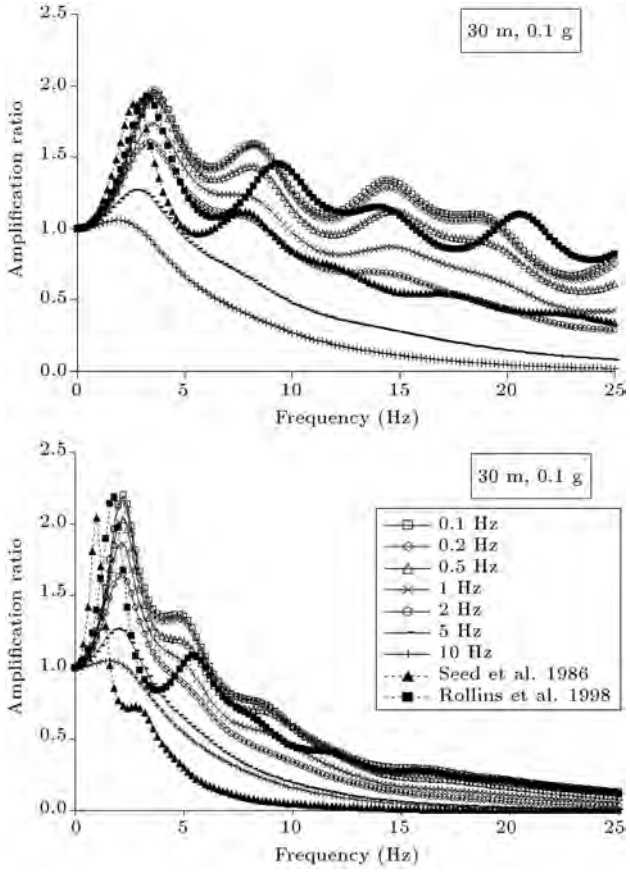

Figure 10. Variation of amplification ratio versus frequency for 30 m thick profile at different loading frequencies under two input base accelerations (i.e. 0.1 and 1 g) for longitudinal component of the 2003 Bam earthquake.

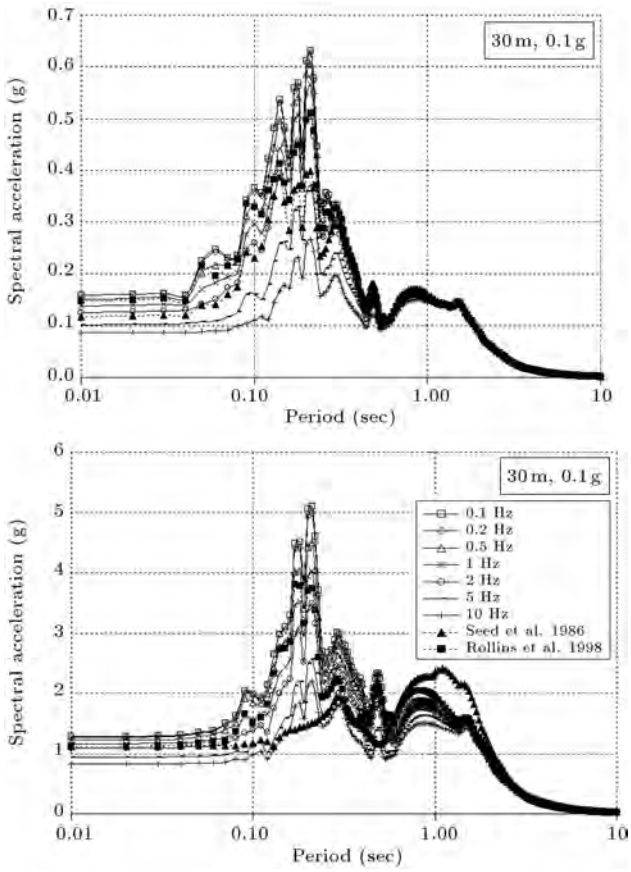

Figure 11. Variation of spectral acceleration versus period for 30 m thick profile at different loading frequencies under two input base accelerations (i.e. 0.1 and 1 g) for longitudinal component of the 2003 Bam earthquake.

strain damping. Figure 10 shows the variation of amplification ratio (defined as the ratio of the amplitude of motion at the top of the seismic bedrock layer divided by that at the top of the first sub-layer) versus frequency for 30 m thick, assuming different G-γ and D-γ curves, obtained for different loading frequencies, under two input base accelerations (i.e. 0.1 g and 1 g), under the longitudinal component of the 2003 Bam earthquake. As shown in Figure 10, with increasing input base acceleration, the maximum amplification ratio at the ground surface has significant, moderate and negligible dependency on the curves of the materials tested, respectively, under the less, near to, and higher than predominant frequency of input motions. Moreover, an increase in input base acceleration causes rapid decrease in the maximum value of amplification at high frequencies, and also causes a decrease in frequency, representing maximum amplification. The maximum amplification decreases as material testing frequency increases.

Figure 11 shows the variation of spectral acceleration versus period for 30 m thick, assuming different G-γ and D-γ curves obtained for different loading frequencies, under two input base accelerations (i.e. 0.1 g and 1 g), under the longitudinal component of the 2003 Bam earthquake. In periods longer than 0.6 s, there is a distinguished peak in the longitudinal component response of the Bam earthquake, and this can be considered its specific characteristic. This fact can be similarly observed in the other lateral component of the Bam Earthquake. Forward rupture directivity and fling-step effects in this strike-slip fault may be responsible for the observed behavior in the fault-normal and fault-parallel directions, respectively [48,49].

In order to attain a better assessment, Figure 12 shows the variation of normalized spectral acceleration (B) versus frequency for a 30 m thick profile at different loading frequencies under two input base accelerations (i.e., 0.1 and 1 g), under the longitudinal component of the 2003 Bam earthquake. As inferred from results, an increase in base input acceleration causes a moderate increase in B factor. This means that the effect of rate-dependent soil behavior is also dependent on the magnitude of input ground motion [34]. For strong ground motion, the soil profile experiences large deformation, a high level of shear strain [34] and, as a

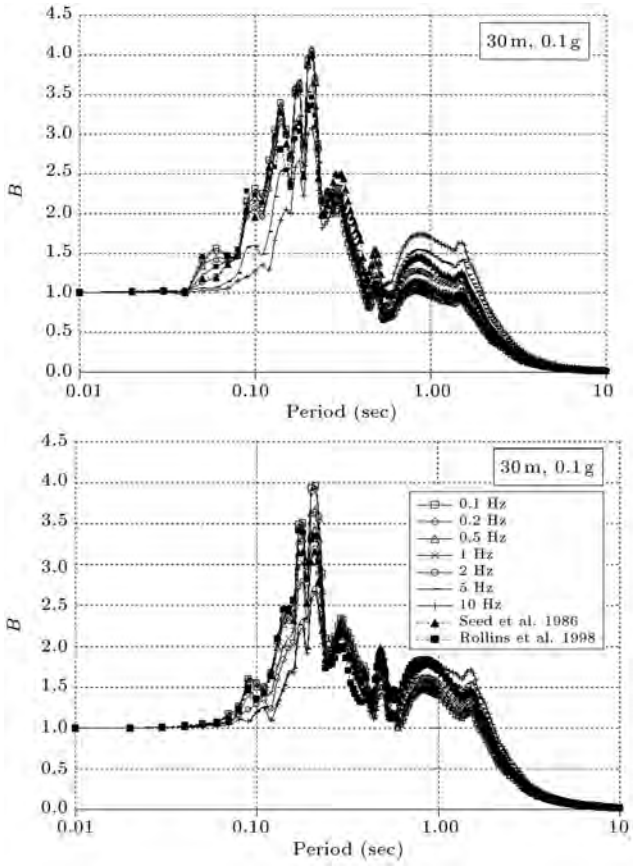

Figure 12. Variation of normalized spectral acceleration (B factor) versus period for 30 m thick profile at different loading frequencies under two input base accelerations (i.e. 0.1 and 1 g) for longitudinal component of the 2003 Bam earthquake.

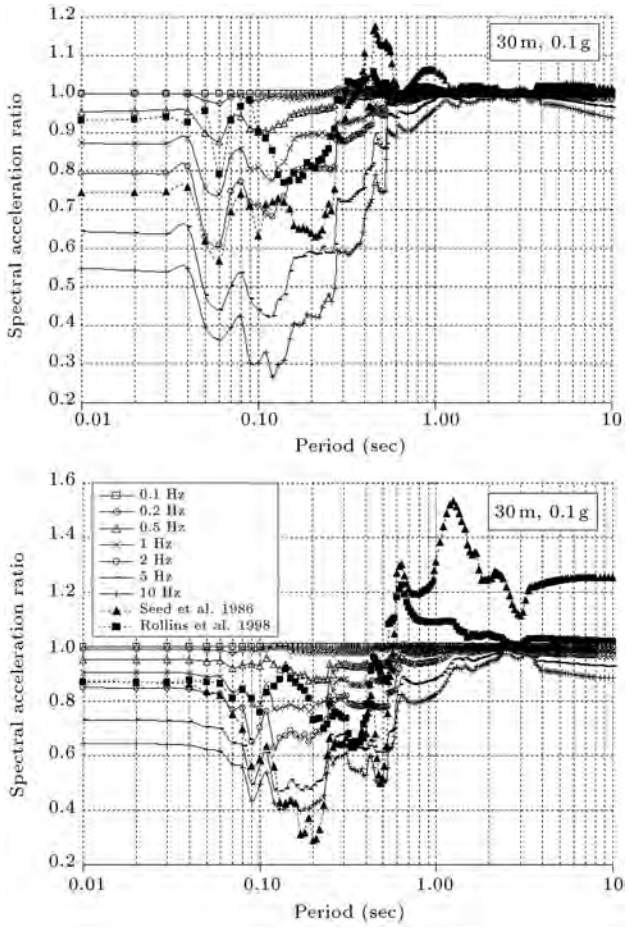

Figure 13. Variation of spectral acceleration ratio versus period for 30 m thick profile at different loading frequencies under two input base accelerations (i.e. 0.1 and 1 g) for longitudinal component of the 2003 Bam earthquake.

result, high rate-dependent damping ratio. Moreover, as loading frequency increases, the B factor, over short and long periods decreases and increases, respectively.

It is noteworthy to mention here that when using the normalized shear modulus and damping proposed by [40,41], the highest B factor is observed at short periods.

Figure 13 shows the calculated response spectrum ratio versus the period for the 30 m thick profile at different loading frequencies at two input base accelerations (i.e., 0.1 and 1 g), using the longitudinal component of the 2003 Bam earthquake. The plots represent the ratios between the frequency-independent and frequency-dependent soil properties. For calculating the spectral acceleration ratio, the reference frequency of the dynamic curve was assumed to be 0.1 Hz. It can be inferred by comparing results presented in Figure 13, where using a frequency higher than the reference frequency of 0.1 Hz results in lower spectral acceleration ratio. So, the effect of frequency-dependent soil behavior on the frequency characteristics of ground motion is dependent on the reference frequency. The high-frequency components (2-10 Hz) are greatly filtered out when the reference frequency is 0.1 Hz, whereas the frequency components between 1 and 10 Hz are highly amplified when the reference frequency is 10 Hz. When comparing the spectral acceleration ratio, using the normalized shear modulus, and damping proposed by [40,41], there is a strange behavior at the period of 0.5 to 2 Hz, where the spectral acceleration ratio is higher than 1. Using these curves in one dimensional response analyses under near fault events may be responsible the high value and narrow band nature of the corresponding spectral at these ranges of periods concerned. Moreover, at the above mentioned periods, the ratios decrease as the base input acceleration increases.

As far as the coincidence of the predominant frequency of the earthquake and the test loading frequency is concerned, as shown in Figure 14(a), the spectral acceleration ratio versus the period for a 30 m thick rockfill (loading frequency of 5 Hz) under maximum base acceleration, at a bedrock of 0.1 g, 0.35 g, and 1 g longitudinal component of the 2003 Bam

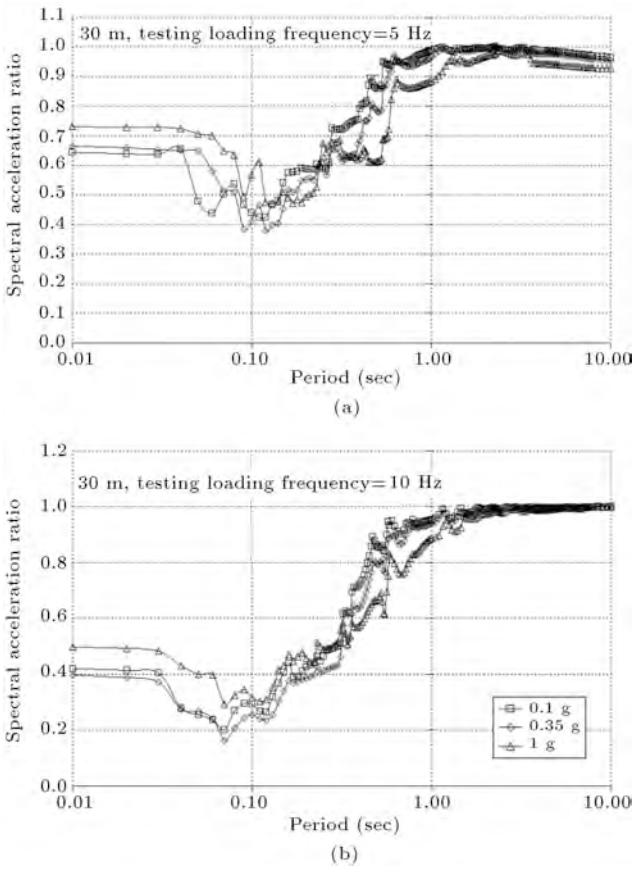

Figure 14. Spectral acceleration ratio versus period for 30 m thick rockfill under maximum base acceleration at bedrock of 0.1 g, 0.35 g, and 1 g longitudinal component of (a) the 2003 Bam earthquake with predominant frequency of 4.862 Hz, and (b) the 1992 Landers earthquake with predominant frequency of 9.4 Hz.

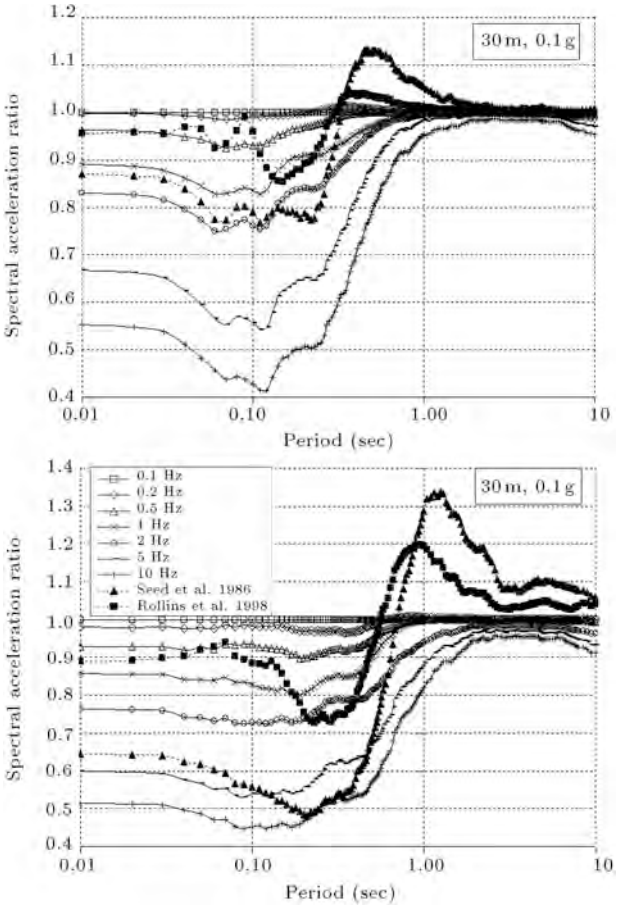

Figure 15. Variation of spectral acceleration ratio versus period for 30 m thick profile at different loading frequencies under two input base accelerations (i.e. 0.1 and 1 g) for all components of selected near fault earthquakes.

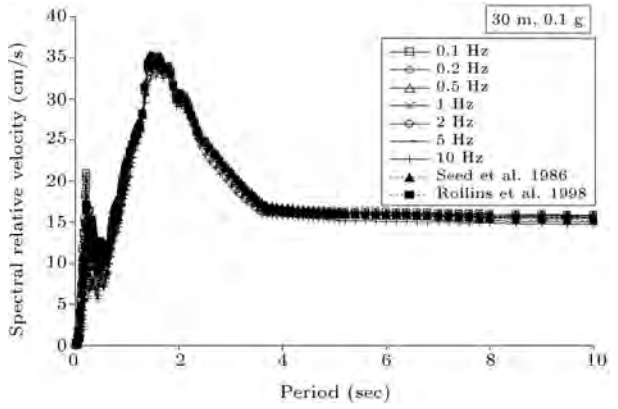

Figure 16. Variation of spectral relative velocity versus period for 30 m thick profile at different loading frequencies under input base acceleration of 0.1 g for longitudinal component of the 2003 Bam earthquake.

earthquake (with predominant frequency of 4.862 Hz), is about 0.38 and 0.47. The relevant values for the Landers earthquake (with a predominant frequency of 9.4 Hz) and material testing frequency of 10 Hz, with respect to base acceleration, range between 0.18 and 0.3 (Figure 14(b)). Hence, selecting the appropriate G and D curves measured at frequencies similar to those of the anticipated cyclic loading (e.g. seismic) is of considerable importance. It can, thus, be concluded that both the amplitude and frequency content of ground motion determine the degree of influence on the rate dependency and propagated near fault ground motion.

Figure 15 shows the calculated response spectrum ratio versus period for a 30 m thick profile at different loading frequencies under two input base accelerations (i.e., 0.1 and 1 g), using all components of selected near fault earthquakes. For calculating spectral acceleration ratio, the reference frequency of the dynamic curve was assumed to be 0.1 Hz, where the loading frequency effect on the response spectrum ratio is evident.

Figure 16, for example, shows the variation of spectral velocity versus period for a 30 m thick profile at different loading frequencies, under the input base acceleration of 0.1 g, under the longitudinal component of the 2003 Bam earthquake. As shown in Figure 16, loading frequency does not have any visible effect on

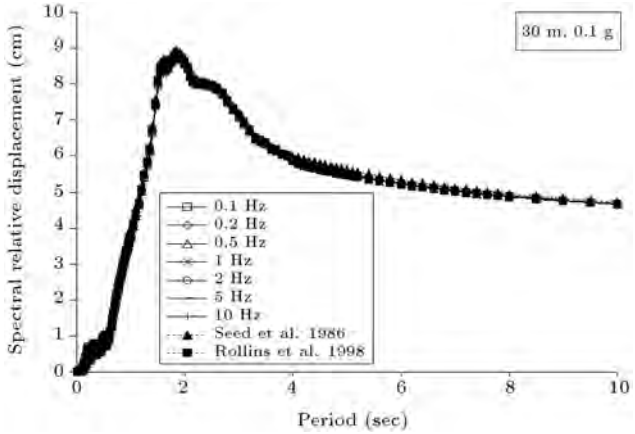

Figure 17. Variation of spectral relative displacement versus period for 30 m thick profile at different loading frequencies under input base acceleration of 0.1 g for longitudinal component of the 2003 Bam earthquake.

spectral relative velocity, either on its value or the period corresponding to the maximum spectral relative velocity. Generally, spectral relative velocity increases as base input acceleration increases, but the loading frequency has negligible effects on the general form of spectral relative velocity.

Figure 17, for example, shows the variation of spectral relative displacement versus period for a 30 m thick profile at different loading frequencies, under input base acceleration of 0.1 g, under the longitudinal component of the 2003 Bam earthquake. As shown, loading frequency does not have any visible effect on spectral relative displacement, either on its value or over the period corresponding to maximum spectral relative displacement. Generally, maximum spectral relative displacement is dependent on base input acceleration and increases as base input acceleration increases, but, the general form of the spectral relative displacement is not affected by loading frequency.

5.2. Results for 90 m thick profile

An identical set of analyses for 90 m thick rockfill, similar to 30 m thick rockfill, was performed to evaluate the effect of the frequency dependency of the shear modulus and strain damping, and the main results are presented in the following. The results of analyses reveal that the amplification ratio for 30 m thick rockfill soil is lower than that of 90 m thick rockfill. Similar results have been reported previously [50].

As far as the coincidence of the predominant frequency of the earthquake and test loading frequency is concerned, as shown in Figure 18(a), the spectral acceleration ratio versus period for 90 m thick rockfill (testing loading frequency of 5 Hz) under maximum base acceleration, at a bedrock of 0.1 g, 0.35 g, and 1 g longitudinal component of the 2003 Bam earthquake (with predominant frequency of 4.862 Hz), is about 0.22-0.27. The relevant values for the Landers

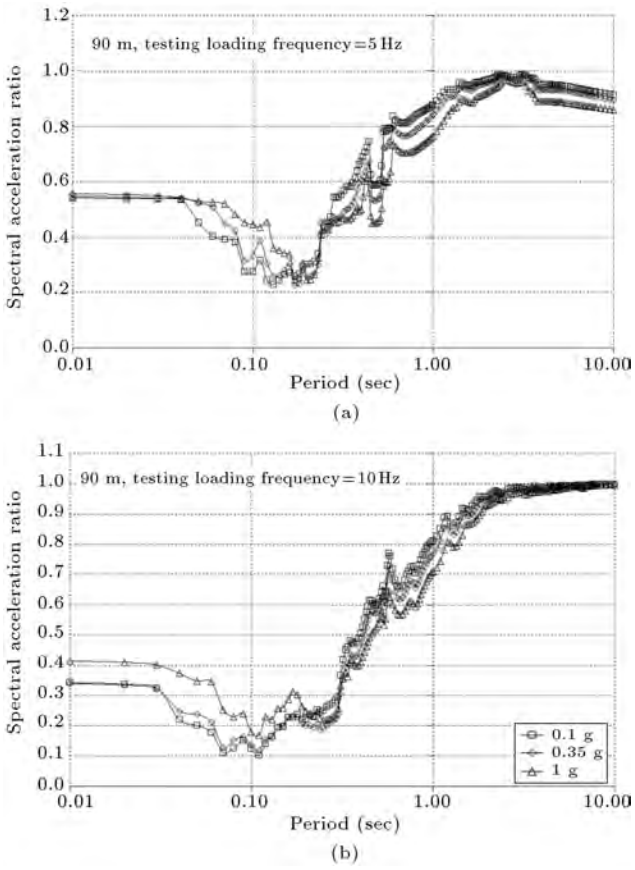

Figure 18. Spectral acceleration ratio versus period for 90 m thick rockfill under maximum base acceleration at bedrock of 0.1 g, 0.35 g and 1 g longitudinal component of (a) the 2003 Bam earthquake with predominant frequency of 4.862 Hz, and (b) the 1992 Landers earthquake with predominant frequency of 9.4 Hz.

earthquake (with a predominant frequency of 9.4 Hz) and material testing frequency of 10 Hz, with respect to base acceleration, range between 0.17 to 0.1 (Figure 18(b)), thus, compared to the 30 m thick profile, the spectral acceleration ratio decreases as the thickness of the soil layer increases. Generally, Chi-Chi and Erzincan motions result in the weakest influence of frequency-dependent soil behavior, and the Landers motion results in a strong influence of frequency dependency. It can thus be concluded that both the amplitude and the frequency content of ground motion determine the degree of influence of frequency dependency.

Figure 19 shows the calculated response spectrum ratio versus period for a 90 m thick profile at different loading frequencies under two input base accelerations (i.e., 0.1 and 1 g), using all components of selected near faults earthquakes. For calculating the spectral acceleration ratio, the reference frequency of the dynamic curve was assumed to be 0.1 Hz, where the loading frequency effect on the response spectrum ratio is evident. The spectral acceleration ratio decreases

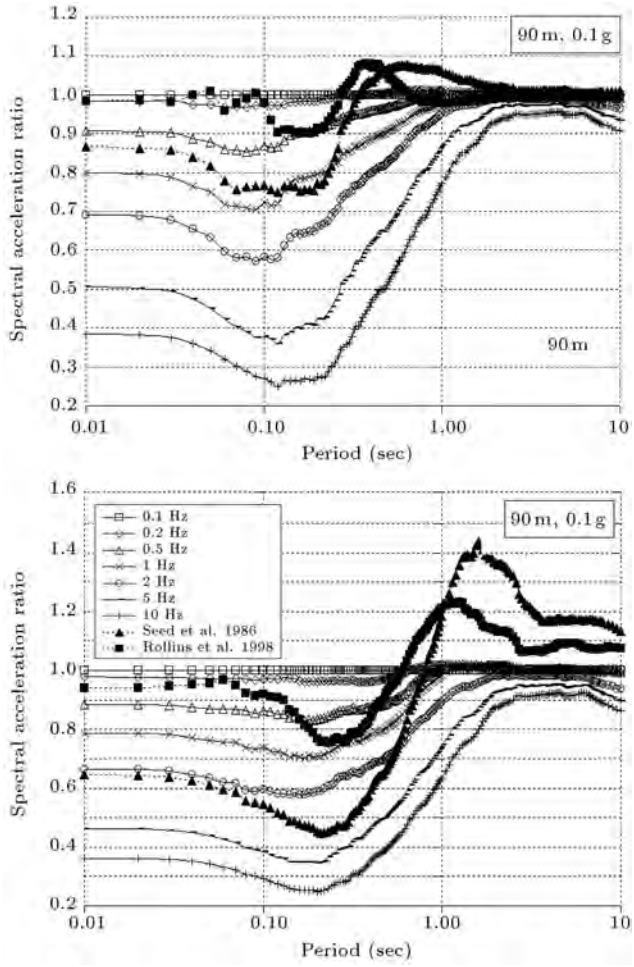

Figure 19. Variation of average spectral acceleration ratio versus period for 90 m thick profile at different loading frequencies under two input base accelerations (i.e. 0.1 and 1 g) for all components of selected near fault earthquakes.

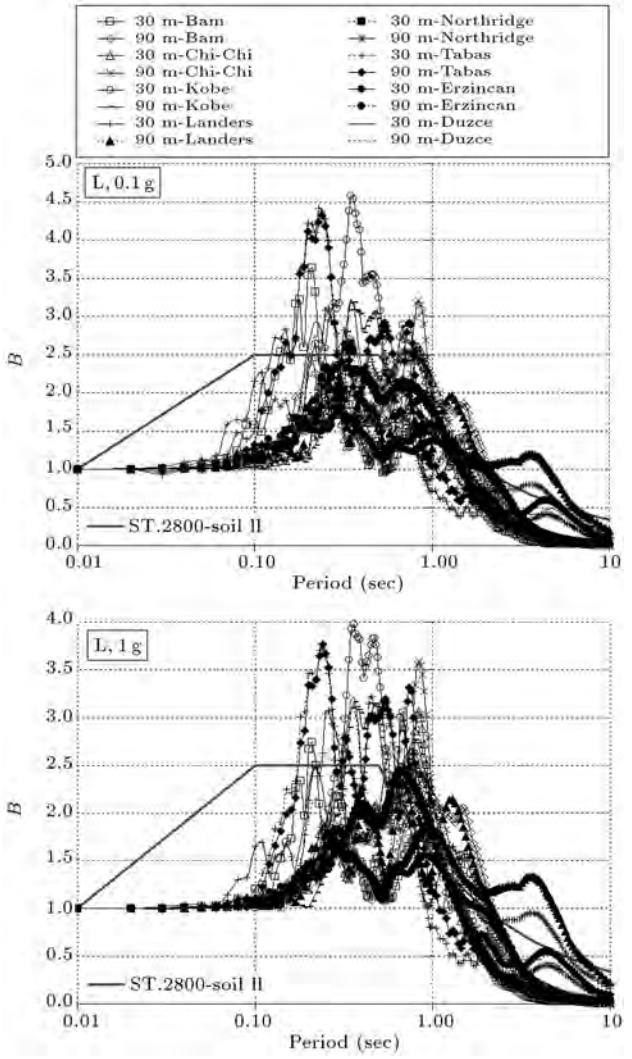

Figure 20. Comparison between the building response factor, B (Standard 2800), and the normalized spectral acceleration versus period for 30 m and 90 m thick profiles at equal predominant frequency under input base acceleration of 0.1 g and 1 g for longitudinal component of used earthquakes.

as the thickness of the soil layer increases. Generally, the use of soil curves obtained at low and high frequencies (compared to the predominant frequency of input motion) results in a calculated frequency-dependent response that is lower and higher than from the frequency-independent analysis, respectively.

Also, according to analyses, an increase in the thickness of the rockfill column does not have a considerable effect on relative velocity and relative displacement.

5.3. Comparison of the response spectra with design spectrum

The high compacted rockfill material studied in this paper is classified as soil numbered II ($375 \leq \bar{V}s(30)$ (m/s)$\leq$ 750) in the design spectra of the Iranian Code of Practice for Seismic Resistant Design of Buildings [43]. This code does not state any specific considerations for construction of buildings near mapped active faults.

Figure 20 shows the variation of normalized spectral acceleration, as well as building response factor, B, [43] versus period for 30 m and 90 m thick profiles under input base acceleration of 0.1 g and 1g for the longitudinal component of selected earthquakes. Based on the predominant frequency of each earthquake, the related soil curves are selected. Maximum calculated normalized spectral acceleration decreases as input base acceleration increases. A similar trend for B has been reported by Standard 2800 [43] for the soil profile type IV, by changing the zone of seismicity from very high to low levels. Generally, the response spectra of the earthquakes and code design spectra do not conform for a wide range of periods. The Ts (the period corresponding to the end portion of the constant spectral acceleration) for a considerable number of

near fault earthquakes (the longitudinal component) are higher than 0.5 s, which is presented in Standard 2800. For 30 m and 90 m thick high compacted rockfill, spectral acceleration at short periods under some near fault earthquakes is higher than $B = 2.5$ of Standard 2800 [43]. These design spectra have a probability of 10% in 50 years, with a return period of 475 years. Since the return period of most of the earthquakes investigated (for example, Bam earthquake) is much longer than that at this risk level, it is normal for the response values to exceed the design spectra, as can be seen in periods between 0.25 and 0.9 s. The degree of influence of frequency-dependent soil behavior at periods higher than 1 s is dependent on the equivalent number of cycles at $0.65\tau_{\max}$ of input ground motion.

Figure 21 shows a comparison between the average normalized spectral acceleration and building response factor, B, [42,43] versus period for 30 m and 90 m thick profiles, under input base accelerations of 0.1 g, 0.35 g and 1 g for longitudinal (L), transversal (T) and vertical (V) components of used earthquakes, under two conditions: (1) As far as the coincidence of the predominant frequency of earthquakes and test loading frequency was concerned, (2) When, for different predominant frequencies of input ground motion, the test loading frequency is 0.1 Hz. It can be seen that test loading frequency, input base acceleration, and thickness of profile have considerable affects on response spectra, especially at short periods (< 1 s).

Nonetheless, it is seen that the UBC [42] design spectra well estimate the response at periods longer than 1 s. It seems that the Iranian Standard 2800 has an un-conservative value at short periods and fairly unsuitable values (overestimate) at long periods.

Figure 22 shows B ratio versus period for 30 m and 90 m thick rockfill (tested at loading frequency of close to predominant frequency of used earthquakes), under maximum base acceleration at a bedrock of 0.1 g, 0.35 g and 1 g for longitudinal, transversal, and vertical

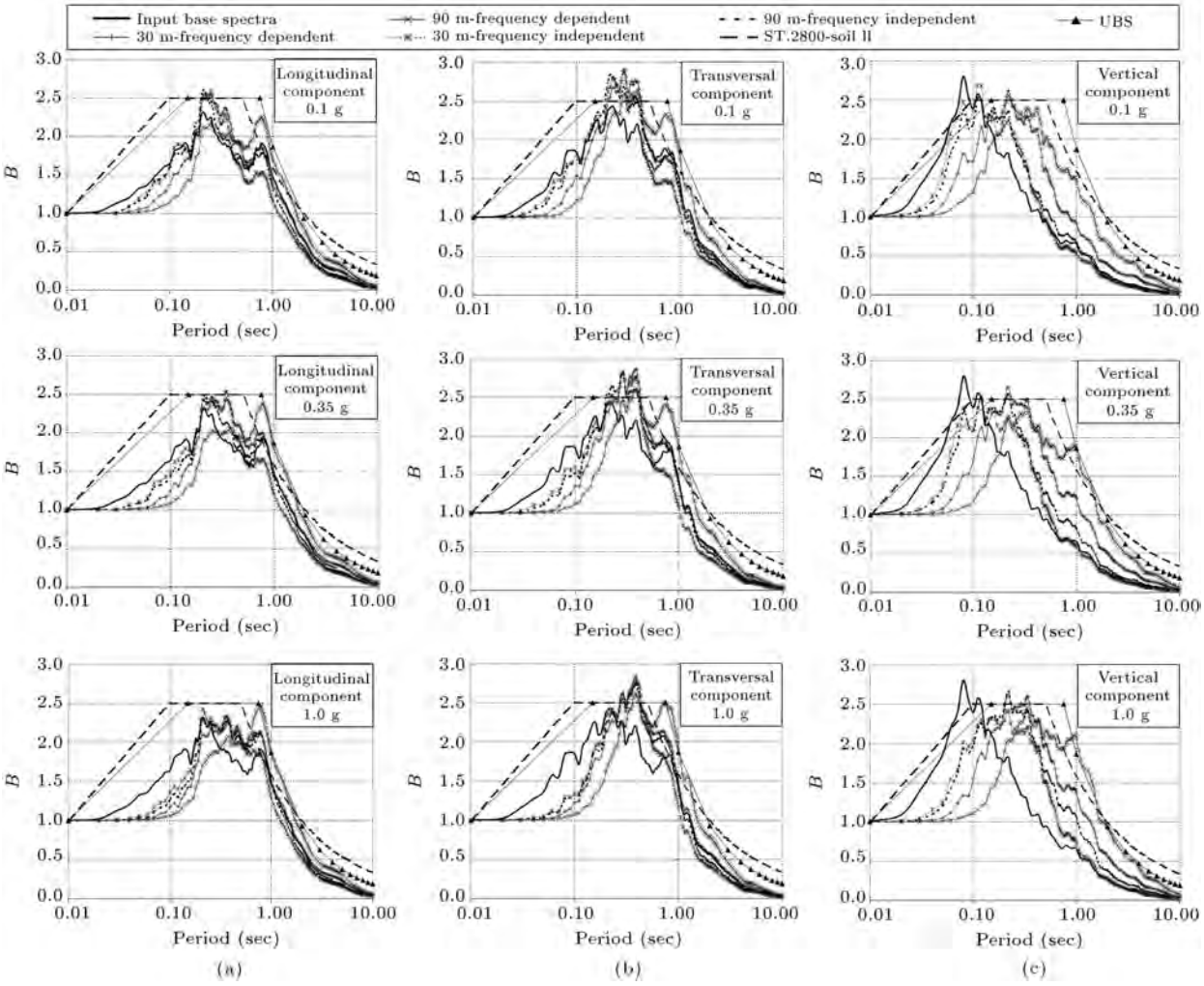

Figure 21. Comparison between the building response factor, B (Standard 2800, UBC), and the average normalized spectral acceleration versus period for 30 m and 90 m thick profiles under input base accelerations of 0.1 g, 0.35 g and 1 g for (a) longitudinal, (b) transversal, and (c) vertical components of used earthquakes.

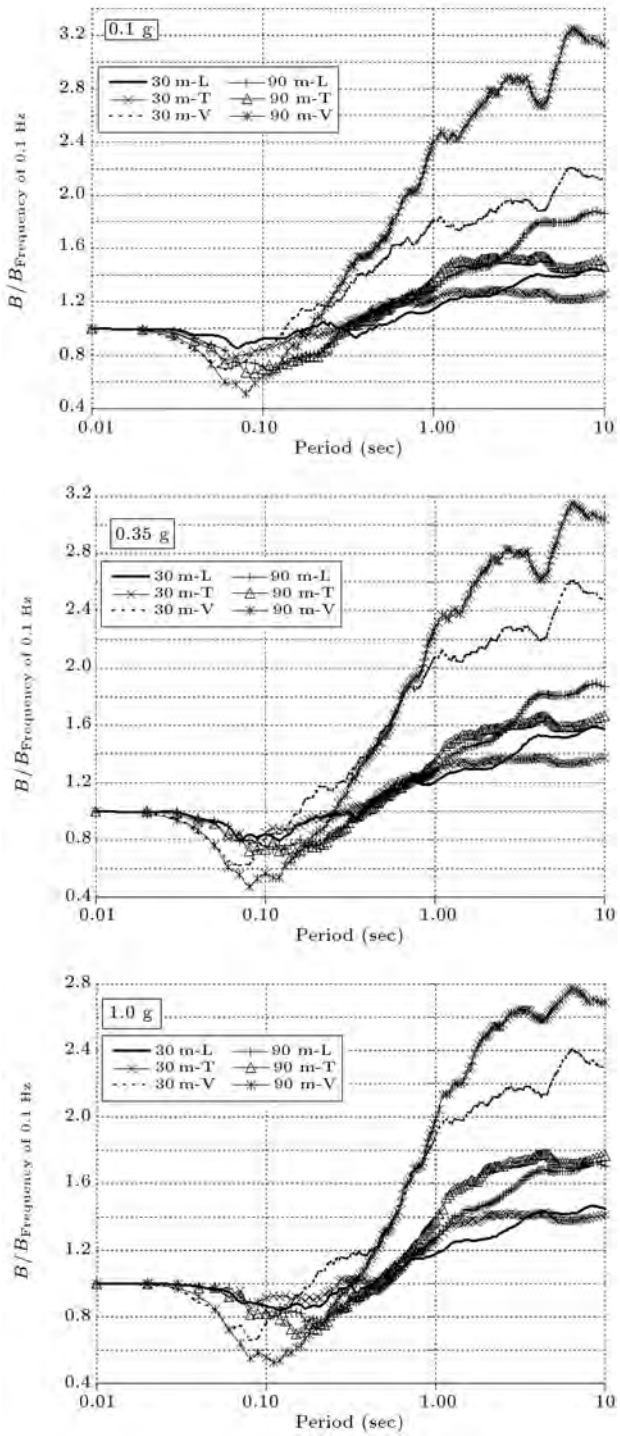

Figure 22. B ratio versus period for 30 m and 90 m thick rockfill (tested at loading frequency close to predominant frequency of the used earthquakes) under maximum base acceleration at bedrock of 0.1 g, 0.35 g and 1 g for longitudinal, transversal and vertical components.

components. For 90 m thickness, low base acceleration and high predominant frequencies, the equivalent linear approach provides smaller B ratio values at the short period. The effect of the frequency-dependent soil behavior at short periods is significant, resulting in

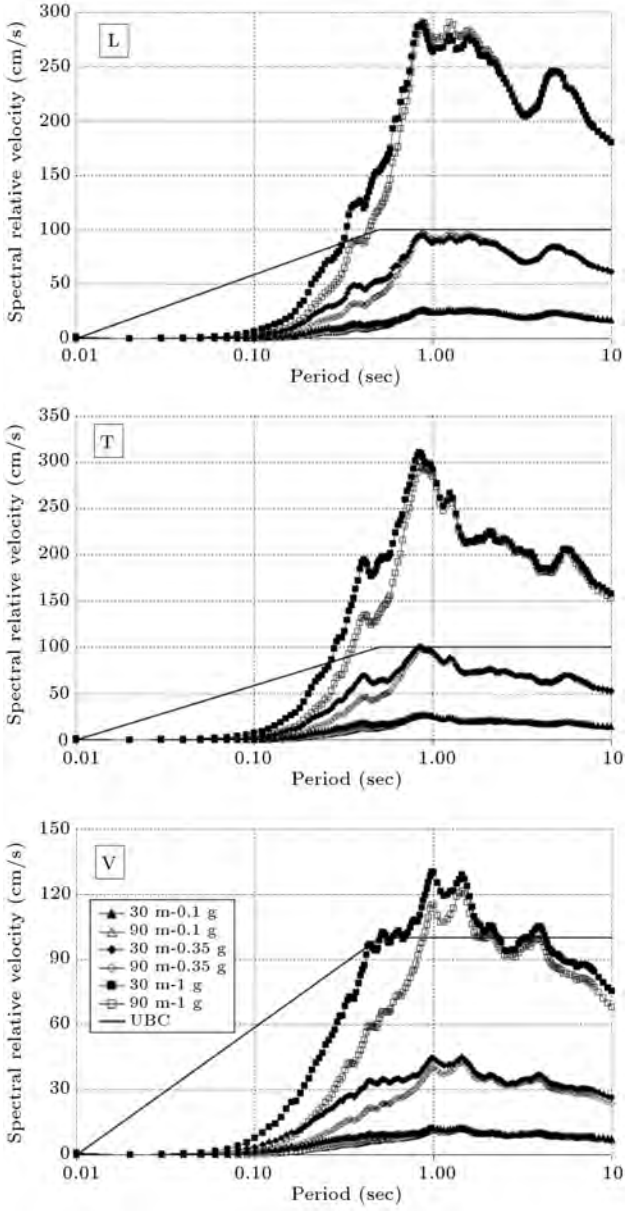

Figure 23. Variation of spectral relative velocity versus period for 30 m and 90 m thick profiles under three input base accelerations (i.e. 0.1, 0.35 and 1 g) for three components of selected near fault earthquakes at testing loading frequency close to predominant frequency of the used earthquakes.

up to 50% difference (average value) in the computed response for used ground motion.

Figures 23 and 24 show the variation of spectral relative velocity and displacement versus period for 30 m and 90 m thick profiles, under three input base accelerations (i.e. 0.1, 0.35 and 1 g) for three components of selected near fault earthquakes, at testing loading frequency close to the predominant frequency of used earthquakes, respectively. The UBC [42] spectral relative velocity and spectral relative displacement are also presented in the figures. The average velocity

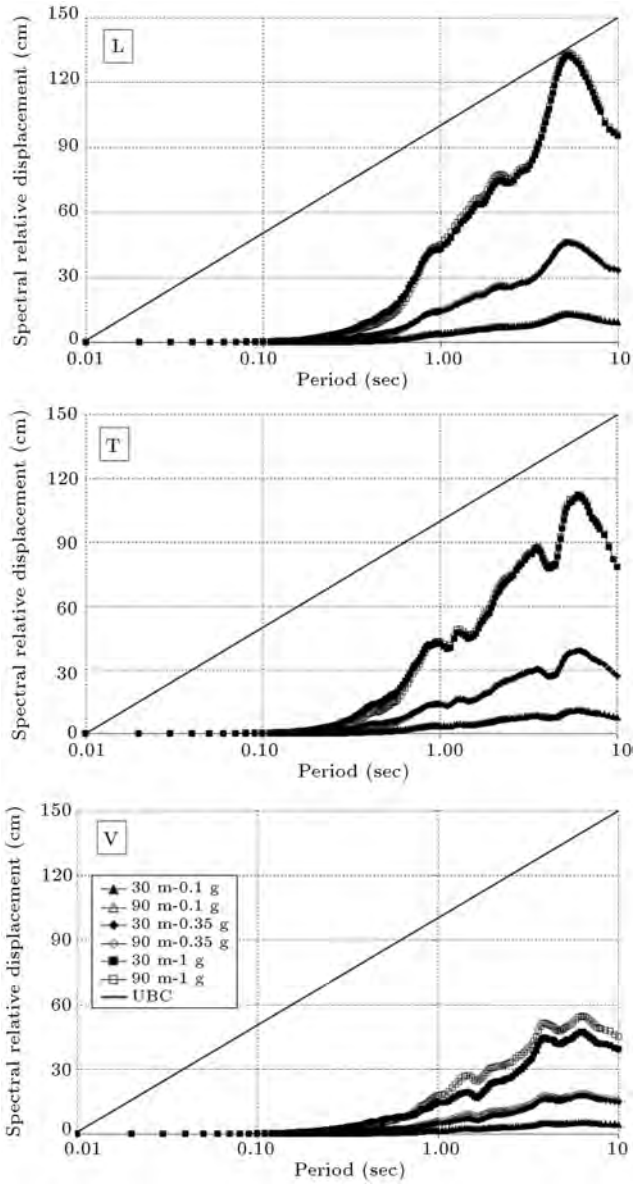

Figure 24. Variation of spectral relative displacement versus period for 30 m and 90 m thick profiles under three input base accelerations (i.e. 0.1, 0.35 and 1 g) for three components of selected near fault earthquakes at testing loading frequency close to predominant frequency of the used earthquakes.

spectra for the vertical components of used earthquakes are compatible with the UBC code spectrum in the low (< 0.8 s) and high (> 2 s) periods under input base acceleration of 1 g, but has a bump in the intermediate period range of 0.8-2 s, where they exceed the UBC code spectrum. Generally, for horizontal components of used earthquakes and base acceleration of 1 g, the spectral relative velocities are higher than UBC ones, especially at periods higher than 0.5 s, but spectral relative displacements lie under the bound suggested by UBC [42]. These results mean that near fault ground motion cannot be adequately described by uniform scaling of a fixed response spectral shape, because the shape of the intermediate-and long-period part of the responses changes as the level of the spectrum increases and as the magnitude increases [47].

5.4. Limitations of the proposed analysis

The reason for considering frequency dependency is because the behavior is considered over the whole duration of the earthquake. Similar to SHAKE, FDEL determines modulus and damping ratio, which are maintained constant throughout the shaking, although each Fourier component has different modulus and damping ratio. Actually, the FDEL technique assigns different material properties to different Fourier series components. It will, therefore, underestimate the frequency dependency for high-frequency components of ground motion, for which small shear strains are expected. It will also overestimate this dependency at strains higher than the effective shear strain in the propagation of a strong ground motion, for which a wide range of strains is expected, and the use of an effective strain to present the frequency dependency of soil behavior at all strain levels becomes less accurate. It is also noted that an equivalent linear method is not an equivalent method to consider earthquake response. The proposed procedure is an approximate solution. More in-depth study is warranted to characterize the accuracy and applicability of the proposed procedure.

6. Conclusions

Based on the published laboratory test results, re-assessment of loading frequency over different materials such as gravelly rockfill materials via laboratory testing is necessary, not only at low strain, but also at medium and higher strains (up to 0.1%). Performing one dimensional site response analysis is useful to account for local site effects at the ground surface, assuming different $G - \gamma$ and $D - \gamma$ curves obtained for different loading frequencies for material under near field earthquake. Frequency dependence in stiffness and damping is shown to appear in the dynamic response, so, it is an advantage in the used frequency-dependent equivalent linear method. Some important findings from the numerical analyses are as follows:

- Generally, the maximum shear strength has higher values at higher frequency, resulting in a higher value of peak acceleration under strong ground motion (this can be attributed to the larger amplification of the motion components characterized by frequencies close to the predominant frequencies of the adopted seismic motion), and the amplification has smaller value at high frequency (de-amplification at the surface may occur). The latter sometimes results in a smaller value of peak acceleration under weak ground shaking.

- Increase in rockfill thickness from 30 m to 90 m causes an increase in amplification ratio, but the spectral acceleration ratio decreases.
- As loading frequency increases, normalized spectral acceleration (B factor) at low and high periods decreases and increases, respectively.
- When comparing the spectral acceleration ratio using the normalized shear modulus and damping proposed by [40,41], there is strange behavior at periods of 0.5 to 2 Hz, where the spectral acceleration ratio is higher than 1. Using these curves in one dimensional response analyses under near fault events may be responsible for the narrow band nature of the corresponding spectral at these ranges of periods. Moreover, at the above mentioned periods, the ratios increase as the base input acceleration increases.

All in all, selection of the appropriate G and D curves measured at a frequency similar to those of the anticipated cyclic loading (e.g. seismic) is of paramount importance. The degree of influence of the frequency-dependent soil behavior is influenced by the thickness of the soil profile, amplitude, equivalent no. of cycles at $0.65\tau_{\max}$, frequency content of input ground motion, and is most significant for higher equivalent no. of cycles at $0.65\tau_{\max}$ of a motion at long periods. Finally, it is important to develop improved representation of the design response spectrum and quantify their impact on structural responses, assuming rate-dependence material behavior under near-fault ground motion.

Acknowledgments

The authors would like to express their gratitude to the Department of Geotechnical Engineering of the Road, Housing and Urban Development Research Center (BHRC), as the project's client, for providing the data and financial support for this research under Grant 1-1775 85 (2008). The open source FDEL technique by Professor N. Yoshida is greatly appreciated. Also, the authors wish to thank the reviewers and referees of this paper for their constructive comments and valuable suggestions.

References

1. Idriss, I.M. and Seed, H.B. "Seismic response of horizontal soil layers", *Journal of the Soil Mechanics and Foundations Division, ASCE*, **94**(4), pp. 1003-1031 (1968).
2. Idriss, I.M. "Response of soft soil sites during earthquakes", In *Proceedings of the Symposium to Honor Professor H.B. Seed*, Berkeley, May, pp. 273-289 (1990).
3. Pavel, F. and Lungu, D. "Correlations between frequency content indicators of strong ground motions and PGV", *Journal of Earthquake Engineering*, **17**(4), pp. 543-559 (2013).
4. Cakir, T. "Evaluation of the effect of earthquake frequency content on seismic behavior of cantilever retaining wall including soil-structure interaction", *Soil Dynamic and Earthquake Engineering*, **45**(2), pp. 96-111 (2013).
5. Sugito, M., Goda, H. and Masuda, T. "Frequency-dependent equ-linearized technique for seismic response analysis of multi-layered ground', *Proceedings of JSCE*, No. 493/III-27, pp. 49-58 (in Japanese) (1994).
6. Sugito, M. "Frequency-dependent equivalent strain for equi-linearized technique", *Proceedings of the First International Conference on Earthquake Geotechnical Engineering*, **1**, A.A. Balkena, Rotterdam, the Netherlands, pp. 655-660 (1995).
7. Yoshida, N., Kobayashi, S., Suetomi, I. and Miura, K. "Equivalent linear method considering frequency dependent characteristics of stiffness and damping", *Soil Dynamics and Earthquake Engineering*, Elsevier, **22**(3), pp. 205-222 (2002).
8. Assimaki, D. and Kausel, E. "An equivalent linear algorithm with frequency and pressure-dependent moduli and damping for the seismic analysis of deep sites", *Soil Dynamics and Earthquake Engineering*, **22**(9-12), pp. 959-965 (2002).
9. Kwak, D.Y., Jeong, C.G., Park, D. and Park, S. "Comparison of frequency-dependent equivalent linear analysis methods", *The 14th World Conference on Earthquake Engineering*, October 12-17, 2008, Beijing, China, **8**, pp. (2008)
10. Idriss, I.M. and Sun, J.I. "User's Manual for SHAKE91. Center for Geotechnical Modeling", Department of Civil Engineering, University of California, Davis (1992).
11. Bardet, J.P., Ichii, K. and Lin, C.H. "EERA, Equivalent linear earthquake site response analysis of layered soils deposits", *User's manual*, University of Southern California, Department of Civil Engineering, August (2000).
12. Ishihara, K.G. *Soil Behavior in Earthquake Engineering*, Clarendon Press, Oxford (1996).
13. Shibuya, S., Mitachi, T., Fukuda, F. and Degoshi, T. "Strain-rate effects on shear modulus and damping of normally consolidated clay", *Geotechnical Testing Journal*, **18**(3), pp. 365-375 (1995).
14. Kazama, M., Toyota, H. and Inutomi, T. "Stress strain relationships in soils directly obtained from centrifuge shaking table tests", *2nd International workshop on Wind and Earthquake Engineering for Offshore and Coastal Facilities* (1995).
15. Zeghal, M., Elgamal, A.W., Tang, H.T. and Stepp, J.C. "Lotung downhole array. II: Evaluation of soil nonlinear properties", *Journal of Geotechnical Engineering, ASCE*, **121**(4), pp. 363-378 (1995).

16. Sundarraj, K.P. "Evaluation of deformation characteristics of 1-g model ground during shaking using a laminar box", Ph.D dissertation, University of Tokyo, Japan (1996).

17. Lai, C.G., Pallara, O., Lo Presti, D.C. and Turco, E. "Low-strain stiffness and material damping ratio coupling in soils", *Advanced Laboratory Stress-Strain Testing of Geomaterials*, T. Tatsuoka, S. Shibuya, and R. Kuwano, Eds., Balkema, Lisse, The Netherlands, pp. 265-274 (2001).

18. Hoque, E. and Tatsuoka, F. "Triaxial system measuring loading-rate effects of sand deformation in cycle", *Geotechnical Testing Journal, ASTM*, **27**(5), pp. 483-495 (2004).

19. Rix, G.J. and Meng, J. "A non-resonance method for measuring dynamic soil properties", *Geotechnical Testing Journal, ASTM*, **28**(1), pp. 1-8 (2005).

20. Brennan, A.J., Thusyanthan, N.I. and Madabhushi, S.P.G. "Evaluation of shear modulus and damping in dynamic centrifuge tests", *Journal of Geotechnical and Geoenvironmental Engineering, ASEC*, **131**(12), pp. 1488-1497 (2005).

21. Kokusho, T., Aoyagi, T. and Wakunami, A. "In-situ soil-specific nonlinear properties back-calculated from vertical array records during 1995 Kobe earthquake", *Journal of Geotechnical and Geoenvironmental Engineering, ASCE*, **131**(11), pp. 1509-1521 (2005).

22. Meng, J. "Earthquake ground motion simulation with frequency-dependent soil properties", *Soil Dynamics and Earthquake Engineering*, Elsevier, **27**, pp. 234-241 (2007).

23. Meza-Fajardo, K.C. and Lai, C.G. "Explicit causal relations between material damping ratio and phase velocity from exact solutions of the dispersion equations of linear viscoelasticity", *Geophysical Journal International*, **171**(3), pp. 1247-1257 (2007).

24. Khan, Z.H., Cascante, G., El Naggar, M.H. and Lai, C.G. "Measurement of frequency-dependent dynamic properties of soils using the resonant-column device", *Journal of Geotechnical and Geoenvironmental Engineering, ASCE*, **134**(9), pp. 1319-1326 (2008).

25. Xenaki, V.C. and Athanasopoulos, G.A.. "Dynamic properties and liquefaction resistance of two soil materials in an earthfill dam-Laboratory test results", *Soil Dynamics and Earthquake Engineering*, **28**, pp. 605-620 (2008).

26. Kallioglou, P., Tika, T.H. and Pitilakis, K. "Shear modulus and damping ratio of cohesive soils", *Journal of Earthquake Engineering*, **12**, pp. 879-913 (2008).

27. Yamada, S., Hyodo, M., Orense, R.P., Dinesh, S.V. and Hyodo, T. "Strain-dependent dynamic properties of remolded sand-clay mixtures", *Journal of Geotechnical and Geoenvironmental Engineering, ASCE*, **134**(7), pp. 972-981 (2008).

28. Karl, L., Haegeman, W., Degrande, G. and Dooms, D. "Determination of the material damping ratio with the bender element test", *Journal of Geotechnical and Geoenvironmental Engineering, ASEC*, **134**(12), pp. 1743-1756 (2008).

29. Aghaei Araei, A., Tabatabaei, S.H. and Ghalandarzadeh, A. "Assessment of shear modulus and damping ratio of gravelly soils", *Research Project*, No 3-4469- 2007, BHRC, Iran (2008).

30. Aghaei Araei, A., Razeghi, H.R., Tabatabaei, S.H. and Ghalandarzadeh, A. "Evaluation of frequency content on properties of gravelly soils", *Research Project*, No. 1-1775-2008, BHRC, Iran (2009).

31. Aghaei Araei, A., Razeghi, H.R., Tabatabaei, S.H. and Ghalandarzadeh, A. "Dynamic properties of gravelly materials", *Scientia Iranica*, **17**(4), pp. 245-261 (2010).

32. Aghaei Araei, A. "Effects of different parameters on dynamic behavior of compacted rockfill materials using large scale triaxial equipment", PhD Thesis, Iran University of Science and Technology (IUST), Iran (2011).

33. Aghaei Araei, A., Razeghi, H.R., Tabatabaei, S.H. and Ghalandarzadeh, A. "Loading frequency effect on stiffness, damping and cyclic strength of modeled rockfill materials", *Soil Dynamics and Earthquake Engineering*, Elsevier, **33**(1), pp. 1-18 (2012), doi.org/10.1016/j.soildyn. 2011.05.009.

34. Aghaei Araei, A., Razeghi, H.R., Ghalandarzadeh, A. and Hashemi Tabatabaei, S. "Effects of loading rate and initial stress state on stress-strain behavior of rock-fill materials under monotonic and cyclic loading conditions", *Scientia Iranica*, **19**(5), pp. 1220-1235 (2012).

35. Watanabe, K. and Kusakabe, O. "Reappraisal of loading rate effects on sand behavior in view of seismic design for pile foundation", *Soils and Foundations*, **53**(2), pp. 215-231 (2013).

36. Park, D. and Hashash, Y.M.A. "Rate-dependent soil behavior in seismic site response analysis", *Canadian Geotechnical Journal*, **45**(4), pp. 454-469 (2008).

37. ASTM D1557. "Standard test methods for laboratory compaction characteristics of soil using modified effort", *Annual Book of ASTM Standard, ASTM International*, West Conshohocken, PA (2003).

38. ASTM Standard D4718-03, 2003: "Practice for correction of unit weight and water content for soils containing oversize particles", *Annual Book of ASTM Standard, ASTM International*, West Conshohocken, PA (2003).

39. ASTM D3999. "Standard test methods for the determination of the modulus and damping properties of soils using the cyclic triaxial apparatus", *Annual Book of ASTM Standard, ASTM International*, West Conshohocken, PA, Re-approved 1996 (2006).

40. Rollins, K.M., Evans, M.D., Diehl, N.B. and Daily, W.D. "Shear modulus and damping relationships for gravels", *Journal of Geotechnical and Geoenvironmental Engineering, ASCE*, **124**(5), pp. 398-405 (1998).

41. Seed, H.B., Wong, R.T., Idriss, I.M. and Tokimatsu, K. "Moduli and damping factors for dynamic analyses of cohesionless soils", *Journal Geotech. Engineering*, **112**(11), pp. 1016-1032 (1986).

42. UBC. *Uniform Building Code*, Handbook (1997).

43. BHRC., *Iranian Code of Practice for Seismic Resistant Design of Buildings (Standard 2800)*, Building and Housing Research Center, 3rd Edition, Tehran, Iran (2005).

44. ASCE. "Minimum design loads for buildings and other structures", ASCE/SEI+7-10 (2010).

45. Schnabel, P.B., Lysmer, J. and Seed, H.B. "SHAKE: A computer program for earthquake response analysis of horizontally layered sites", Report No. UCB/EERC-72/12, Earthquake Engineering Research Center, University of California, Berkeley, December, 102 p (1972).

46. Pacific Earthquake Engineering Research Center, "PEER strong motion database" (2008) http://peer.berkeley.edu/smcat/.

47. Seed, H.B., Idriss, I.M., Makdisi, F. and Banerjee, N. "Representation of irregular stress-time history by equivalent uniform stress in liquefaction analysis", Report No. EERC 75-29, Earthquake Engineering Research Center, University of California, Berkeley (1975).

48. Somerville, P. "Magnitude scaling of near fault rupture directivity pulse", *Physics of Earth and Planetary Interiors*, **137**, pp. 201-212 (2003).

49. Tang, Y. and Zhang, J. "Response spectrum-oriented pulse identification and magnitude scaling of forward directivity pulses in near-fault ground motions", *Dynamics and Earthquake Engineering*, **31**, pp. 59-76 (2011).

50. Rodriguez-Marek, A. and Bray, J.D. "Seismic site response for near-fault forward directivity ground motions", *Journal of Geotechnical and Geoenvironmental Engineering, ASCE*, **132**(12), pp. 1611-1620 (2006).

Biographies

Hamid Reza Rezeghi received his PhD degree from Tohoku University, Japan, in 2000, and is now Associate Professor in the School of Civil Engineering at Iran University of Science and Technology, Iran. His research interests include geotechnical and geoenvironmental engineering.

Ata Aghaei Araei received his PhD degree from Iran University of Science and Technology (IUST), Iran, in 2011 (he was PhD researcher at the Geotechnical Laboratory of Civil Engineering at The University of Tokyo, Japan). He is Assistance Professor in the Road, Housing and Urban Development Research Center (BHRC), Iran, where he is working as Senior Geotechnical Engineer and Head of the Geotechnical Laboratory. His primary research interests include monotonic and dynamic testing on geomaterials, microzonation, and geotechnical equipment construction.

Abbas Ghalandarzadeh received his PhD degree in Geotechnical Engineering from the University of Tokyo in 1997, and is currently Associate Professor School of Civil Engineering at the University of Tehran, Iran, where he is Head of the Soil Mechanics and Centrifuge Laboratory. He is member of the Technical Committee of TC2 of the International Society of Soil Mechanics and Geotechnical Engineering. His research interests are mainly in the area of experimental geotechnics, particularly in model and element testing, and also earthquake geotechnical engineering, including the dynamic behavior of rockfill dams with asphalt concrete cores, the seismic behavior of quay walls, reinforced earth and piles, and more recently the anisotropic behavior of saturated sands mixed with clay or silt.

Saeid Hashemi Tabatabaei received his PhD degree from Roorkee University, India, in 1992, and is currently Associate Professor in the Road, Housing and Urban Development Research Center (BHRC). He has over 18 years experience in the field of geotechnical engineering and geotechnical engineering research. He has been involved in over 33 engineering projects in the fields of landslide hazard and risk assessment, slope stability analysis and mitigation, soil improvement, engineering geological mapping for microzonation of rural areas, and site investigation.